Exploring how the fast-slow pace of life continuum and cell size structure microorganism life history variation

Josje Romeijn[1] & Isabel M. Smallegange[2]

[1] Institute for Biodiversity and Ecosystem Dynamics, University of Amsterdam, PO Box 94240, 1090 GE Amsterdam, The Netherlands

[2] School of Natural & Environmental Sciences, Newcastle University, Newcastle upon Tyne, NE1 7RU, UK

Corresponding author: Isabel M. Smallegange – Isabel.smallegange@newcastle.ac.uk

Abstract

Identifying patterns in life history strategies has proven essential to predict how macro-organisms respond to disturbances and stressors. Like macro-organisms, microorganisms display a wide range of growth, cell division and reproduction patterns, but, unlike for macro-organisms, we know little of what determinants structure microorganism life history variation. We used four life history traits that determine growth and reproduction – the von Bertalanffy growth rate, cell length at birth, maximum length, and length at cell division – of 13 microorganisms (bacteria, fungi, a protist and plant) to parameterise a dynamic energy budget integral projection model for each species to calculate its generation time, mean lifetime reproductive success, and population growth rate. Inputting all values into a phylogenetically informed principal component analysis, we show that 91% of microorganism life-history variation falls along two independent axes. Like macro-organisms, we find a fast–slow pace of life continuum, including faster-growing, shorter-lived microorganisms at one end, and slower-growing, longer-lived microorganisms at the other. Unlike macro-organisms, we find a second, size-at-life-stage axis, with microorganisms with shorter birth, division and maximum cell length at one end, and microorganisms with longer lengths at the other. We advocate that this pilot study of structuring microorganism life history variation can ignite future life history research to understand the diversity of microorganismal phenotypes. Such endeavours can aid predictions on how microorganisms respond to disturbances, especially if more complex cell growth and division processes are incorporated.

Keywords: demography, fast-slow continuum, life history strategies, matrix model, microbes, yeast

Introduction

Species responses to changes in their environment are mediated by their demographic schedules of survival, growth, and reproduction, which comprise life-history strategies. Because life history strategies are related to population performance and rate of recovery from disturbance (Salguero-Gómez et al., 2016; Paniw et al., 2018; Capdevila et al., 2020), a first step to predict population responses to environmental change is to classify species by their life history strategy (Gaillard et al., 2016; Smallegange et al., 2020). For example, in animals and plants, the majority of life history variation is structured along (i) a fast-slow life history continuum with fast-growing, short-lived species at one end, and slow-growing, long-lived species at the other (Gaillard et al., 1989; Paniw et al., 2018; Capdevila et al., 2020), and (ii) a reproductive strategy axis that for plants has iteroparous species at one end and semelparous plants at the other (Salguero-Gómez et al., 2016; Paniw et al., 2018), whereas for animals this axis is defined by the distribution of age-specific mortality hazards and the spread of reproduction (Healy et al., 2019).

Microorganisms are typically classified along a copiotroph-oligotroph dichotomy (Koch 2001), where copiotrophs grow faster and rely on resource availability, but oligotrophs efficiently exploit resource at the expense of growth rate (note that Ramin and Allison (2019) added a third, maintenance type). It is not clear, however, if microorganismal life history variation can be structured along the fast-slow life history continuum, or along an axis of reproductive strategies (Evans and Wallenstein 2013). Such knowledge can, however, be useful because processes influenced by microorganisms, e.g., human disease progression (de Vrieze et al., 2013), human-microbe interactions (Rook et al., 2017) and even ecological strategies of coral species (Meistertzheim et al., 2016), are driven by population dynamics at the microbial level that can be affected differently by different life history strategies.

The aim of this pilot study is to explore main axes of variation in microorganism life histories to ignite further research on microbial life history strategies. We adapted a dynamic energy budget integral projection model (DEB-IPM) (Smallegange et al., 2017) to the microorganism life cycle, in

which individuals show von Bertalanffy cell growth and reproduce by binary fission to produce two offspring (Margolin 2005) after which individuals die. We parameterised DEB-IPMs for 13 species of microorganism, including bacteria, fungi, a plant and a protist to calculate each species' population growth rate λ, mean lifetime reproductive success R_0, and generation time T. We performed a phylogenetically informed principal component analysis (PCA) on the latter quantities and the species traits cell length at birth, cell length at division, maximum cell length and von Bertalanffy growth rate to classify microorganisms according to main life history strategies.

Methods

Brief description of the DEB-IPM

Four fundamental functions describe how an individual microorganism moves through its life cycle: the survival function, $S(L(t))$, the growth function, $G(L', L(t))$, the reproduction function, $R\big(L(t)\big)$, and the parent-offspring function, $D(L', L(t))$, which describes the association between the cell length of the parent L and offspring cell length L'. Denoting the number of microorganisms at time t by $N(L, t)$ gives the dynamics of the cell length number distribution from time t to t+1 as:

$$N(L', t+1) = \int_{\Omega} \left[D(L', L(t))R\big(L(t)\big) + G(L', L(t))S(L(t))\right]N(L, t)dL \qquad \text{eqn 1}$$

where the closed interval Ω denotes the cell length domain. Note that this simple DEB-IPM does not account for temperature effects or reserve dynamics (which can, however, be an acceptable simplification [Jager et al. 2013]).

The survival function $S(L(t))$ is the probability that an individual of cell length L survives from time t to t + 1:

$$S(L(t)) = \begin{cases} (1 - p_D)e^{-\mu} & \text{for } L \leq L_m E(Y)/\kappa \\ 0 & \text{otherwise.} \end{cases} \qquad \text{eqn 2}$$

assuming a constant background mortality rate μ. The parameter L_m is the maximum cell length under conditions of unlimited abundance of food of the highest, relative quality, $E(Y) = 1$, and κ is the fraction of ingested energy allocated to respiration. The probability of an individual dividing to produce $n_O = 2$ offspring, p_D, enters the survival function to represent binary fission (Margolin 2005), because reproduction in microorganisms entails that the dividing individual ceases to exist. Individuals die from starvation at a cell length at which maintenance requirements exceed the total amount of assimilated energy, which occurs when $L > L_m \cdot E(Y)/\kappa$ and hence, then, $S\big(L(t)\big) = 0$ (e.g., an individual of size L_m will die of starvation if $E(Y) < \kappa$).

The function $G(L', L(t))$ is the probability that an individual of cell length L at time t grows to length L' at $t + 1$, conditional on survival, and follows a Gaussian distribution (Easterling et al., 2000):

$$G(L', L(t)) = \frac{1}{\sqrt{2\pi\sigma_L(L(t+1))}} e^{\frac{-(L' - E(L(t+1))^2}{2\sigma_L^2(L(t+1))}} \qquad \text{eqn 3}$$

with

$$E\big(L(t+1)\big) = L(t)e^{-\dot{r}_B} + \big(1 - e^{-\dot{r}_B}\big)L_m \cdot E(Y), \qquad \text{eqn 4}$$

and

$$\sigma^2(L(t+1)) = (1 - e^{-\dot{r}_B})^2 L_m^2 \sigma^2(Y), \qquad \text{eqn 5}$$

where $\dot{r}_B$ is the von Bertalanffy growth rate and $\sigma(Y)$ is the standard deviation of the expected feeding level, assuming individuals can shrink under starvation conditions.

The reproduction function $R(L(t))$ gives the number of offspring produced between time t and $t + 1$ by an individual of cell length L at time t:

$$R(L(t)) = \begin{cases} 0 & \text{for } L_b \leq L < L_d \\ n_O \cdot p_D & \text{for } L_d \leq L \leq L_m E(Y)/\kappa \end{cases} \qquad \text{eqn 6}$$

We set the cell length at which individuals divide, L_d, equal to the asymptote of the von Bertalanffy growth curve in cell length so that $L_d = E(Y) \cdot L_m$. Only surviving adults reproduce; thus, only individuals within a cohort of cell length $L_d \leq L \leq L_m Y/\kappa$ reproduce. The probability of an individual dividing, p_D, equals:

$$p_D = \begin{cases} 0 & \text{for } L < L_d \\ 1 & \text{for } L \geq L_d \end{cases} \qquad \text{eqn 7}$$

The probability density function $D(L', L(t))$ gives the probability that the offspring of an individual of cell length L are of length L' at time $t + 1$:

$$D\big(L', L(t)\big) = \begin{cases} 0 & \text{for } L < L_d \\ \frac{1}{\sqrt{2\pi\sigma^2_{L_b}(L(t))}} e^{\frac{-(L' - E_{L_b}(L(t)))^2}{2\sigma^2_{L_b}(L(t))}} & \text{otherwise} \end{cases} \qquad \text{eqn 8}$$

where $E_{L_b}\big(L(t)\big)$ is the expected cell length of offspring produced by a cohort of individuals with length $L(t)$, and $\sigma^2_{L_b}(L(t))$ the associated variance. For simplicity, we set $E_{L_b}\big(L(t)\big) = L_b$ constant, and assumed its associated variance, $\sigma^2_{L_b}\big(L(t)\big)$, to be negligibly small.

113 **Parameterization of the DEB-IPM**

114 We parameterized DEB-IPMs for 13 microorganisms (Fig. 1A) (Table 1), setting κ, μ and n_0 at

115 constant values: $\kappa = 0.9$ (assuming most energy goes to respiration), $\mu = 0.01$ h^{-1} (assuming

116 background mortality under laboratory circumstances is very low), and $n_O = 2$ (as one microorganism

117 divides to produce two offspring) (Table 1). Values of L_b, L_d, L_m, and $\dot{r}_B$ were taken from the literature

118 (references in Table 1) or estimated from other data (explained in Table 1). We did not take

119 parameter values from mutants, knock-out variants, or microorganisms kept under starvation

120 conditions.

121

122 **Identifying life history patterns**

123 We first calculated the population growth rate (λ), mean lifetime reproductive success (R_0) and

124 generation time (T) from each DEB-IPM (see MatLab code in Supplementary Material [MATLAB.

125 version 9.2.0.556344 R2017a]). We set $E(Y)$ for each species such that it mimics favourable

126 laboratory conditions and exponential growth, so that $\lambda > 1$ and $R_0 > 1$ (Table 2). We discretised the

127 IPM (Eqn 1) by dividing the length domain Ω into 200 very small-width discrete bins, resulting in a

128 matrix, which dominant eigenvalue equals λ. R_0 was the dominant eigenvalue of the matrix

129 $\mathbf{F} = \mathbf{V}(\mathbf{I} - \mathbf{GS})^{-1}$, where **I** is the identity matrix and **V** = **DR**, with **D** as the parent-offspring

130 association, **R** the reproduction, **G** the growth and **S** the survival matrix (Caswell 2001). Generation

131 time $T = \log(R_0)/\log(\lambda)$ (Caswell 2001). We then performed a varimax-rotated, phylogenetically

132 informed PCA on all values of L_b, L_d, L_m, $\dot{r}_B$, λ, R_0, and T (Tables 1 & 2) in R (R Core Team 2021) using

133 the *phyl.pca* function in the R library *phytools* (Revell 2012; Salguero-Gómez et al., 2016; Paniw et al.

134 2018) (see R code in Supplementary Material), after log-transforming and scaling values to $\mu = 0$ and

135 SD = 1 to agree with PCA assumptions. We estimated Pagel's λ to inform on the phylogenetic

136 correlation between species (Freckleton et al., 2002), which varies between 0 (phylogenetic

137 independence) and 1 (species traits covary proportionally to their shared evolutionary history).

138 Significance of PCA axes was assessed using Kaiser's criterion [Legendre and Legendre, 2012]).

Results

Population growth was predicted for all species ($\lambda > 1$; $R_0 > 1$), with generation time T ranging from just over two hours (*B. subtilis* and *C. vibrioides*) to 36 hours (*S. elongatus*) and almost 80 hours (*C. reinhardtii*) (Table 2). We further found that two variance-maximised, rotated PCA axes explained 91% of variation in the life history traits (Fig. 1B). The first PCA axis captured the position of the species along a slow-fast pace of life continuum, with high positive loadings for $\dot{r}_B$, λ and R_0 and a high negative loading of T (Fig. 1B). The second PCA axis captured variation in size-at-life-stage, with large negative loadings corresponding to species that have large L_b, L_d and L_m (Fig. 1B). There was no phylogenetic signature in the structuring of life history variation (Pagel's λ was almost zero: λ = 0.000069).

Discussion

Life history theory is used to classify animals and plants by their life history strategy to better understand how populations respond to environmental change, disturbances, and stressors (Salguero-Gómez et al., 2016; Paniw et al., 2018; Capdevila et al., 2020; Smallegange et al., 2020). Like animals and plants, we found that microorganismal life history variation was unaffected by phylogeny and structured along a fast-slow pace of life continuum, which represents a trade-off between survival and reproduction (Gaillard et al., 2016; Salguero-Gómez et al., 2016). However, unlike animals or plants (Salguero-Gómez et al., 2016; Paniw et al., 2018), we found that the second axis did not represent reproductive strategies but reflected size-at-life-stage. This is perhaps not surprising as we *a priori* fixed reproduction for all species to reflect binary fission (always producing two offspring), but selected species that covered a wide range in cell growth patterns.

Growth patterns of bacteria and other microorganisms are often categorised as following a timer, sizer or an adder model, depending on what mechanism triggers cell division (Campos et al.,

165 2014; Taheri-Araghi et al., 2015; Sauls et al., 2016). Under equilibrium conditions, both the sizer and
166 adder model result in asexual cell division at a fixed size (Sauls et al., 2016), like in our model.
167 However, of the species that we studied, the plant *C. reinhardtii*, the fungi *S. pombe* and *S.*
168 *cerevisiae*, and the protist *D. discoideum* can reproduce sexually (Nielsen 2004; Urushihara and
169 Muramoto, 2006; Wallen and Perlin, 2018). Also, when reproducing asexually, *S. cerevisiae* divides
170 via budding, producing a smaller offspring cell and a remaining, larger parent cell. The plant *C.*
171 *reinhardtii*, in turn, undergoes a multiple-fission cycle, potentially producing up to eight daughter
172 cells (Cross and Umen, 2015). Future endeavours could explore how these more complex growth
173 and reproduction patterns affect life history patterning.

174 Lastly, we standardised cell growth across species by setting the expected feeding level, $E(Y)$,
175 at a level that simulated favourable conditions and exponential growth. Yet, *S. cerevisiae* and *B.*
176 *subtilis* can show great plasticity in their life history trajectories because their cell growth depends
177 on food quality (Ferrezuelo et al., 2012; Sauls et al., 2019). If such intraspecific variation is greater
178 than variation in growth between species, it will challenge the detection of broad-scale patterns in
179 life histories across species (Pottor et al. 2021). It will thus be interesting to explore if microbial life
180 history variation can be structured in variable environments, in which growth depends on
181 environmental quality (Smallegange et al. 2014).

182 In conclusion, like macro-organisms, microorganisms have phenotypic traits that influence
183 growth and that are subject to tradeoffs (Ramin & Allison, 2019). Also, like macro-organisms,
184 microorganisms are exposed to different environmental disturbances and selection pressures that
185 can drive the evolution of a wide range of life history strategies. We identified two axes of life
186 history variation in microorganisms for a small set of species. Next steps should at least (i) target
187 more species, including from the field, (ii) systematically control abiotic factors like temperature, (iii)
188 explore a variety of growth and reproduction patterns and (iv) assess if microbial life history
189 strategies inform on sensitivity to environmental change. We hope that our first exploration will
190 ignite such research. It will help us understand the diversity of microorganismal phenotypes (Keymer

et al., 2006; Santillan et al., 2019; Kiørboe & Thomas, 2020), and increase our understanding of how they impact on higher level processes like host phenotype expression (Kopecky et al., 2014; Zindel et al., 2017), and human health (de Vrieze et al., 2013; Rook et al., 2017).

Author contributions

Isabel M. Smallegange: conceptualisation, supervision and writing of final draft. **Josje Romeijn**: data collection, formal analysis, visualisation, and writing of the first draft.

Data availability statement

Supplemental data, R code and MatLab code is available at https://doi.org/10.6084/m9.figshare.16831543.v1.

References

Aldridge, B. et al. 2011. Asymmetry and aging of mycobacterial cells lead to variable growth and antibiotic susceptibility. - Science 335: 100–104.

Allard, C. et al. 2018. A size-invariant bud-duration timer enables robustness in yeast cell size control. – PloS One 13: e0209301

Banerjee, S. et al. 2017. Biphasic growth dynamics control cell division in *Caulobacter crescentus*. - Nature Microbiology 2: 17116.

Beaufay, F et al. (2015). A NAD-dependent glutamate dehydrogenase coordinates metabolism with cell division in *Caulobacter crescentus*. - The EMBO journal, 34: 1786-1800.

Buchwald, P. and Sveiczer, A. (2006). The time-profile of cell growth in fission yeast: Model selection criteria favoring bilinear models over exponential ones. - Theor. Biol. Med. Mod. 3:16.

Campos, M. et al. 2014. A constant size extension drives bacterial cell size homeostasis. – Cell 159:1433-1446.

Capdevilla, P. 2020. Longevity, body dimension and reproductive mode drive differences in aquatic versus terrestrial life history strategies. – Funct. Ecol. 34: 1613–1625.

Caswell, H. 2001. Matrix Population Models. Sunderland, MA: Sinauer Associates.

Chamberlain, S. andSzocs, E. 2013. taxize - taxonomic search and retrieval in R. - F1000Research 2: 191.

Cross, F. and Umen, J. 2015. The chlamydomonas cell cycle. - Plant J. 82: 370-392.

Deforet, M. et al. 2015. Cell-size homeostasis and the incremental rule in a bacterial pathogen. - Biophys. J. 109: 521–528.

Evans, S. and Wallenstein, M. 2013. Climate change alters ecological strategies of soil bacteria. - Ecol. Lett. 17: 155-164.

Ferrezuelo, F. et al. 2012. The critical size is set at a single-cell level by growth rate to attain homeostasis and adaptation. - Nature Comm. 3: 1012.

Fiévet, A. 2015. Single-cell analysis of growth and cell division of the anaerobe *Desulfovibrio vulgaris* Hildenborough. - Front Microbiol. 6: 1378.

Freckleton, R.P. et al. 2002. Phylogenetic analysis and comparative data: a test and review of evidence. – Am. Nat. 160: 712–726.

Gaillard, J.-M. et al. 1989. An analysis of demographic tactics in birds and mammals. - Oikos 56: 59–76.

Healy, K. et al. 2019. Animal life history is shaped by the pace of life and the distribution of age-specific mortality and reproduction. - Nature Ecol. Evol. 3: 1217-1224.

Hinchliff, C.E. et al. 2015. Synthesis of phylogeny and taxonomy into a comprehensive tree of life. – Proc. Natl. Acad. Sci. USA 112: 201423041.

Jager, T. et al. 2013. DEBkiss or the quest for the simplest generic model of animal life history. - J. Theor. Biol. 328:9-18.

Kiørboe, T. and Thomas, M.K. 2020. Heterotrophic eukaryotes show a slow-fast continuum, not a gleaner–exploiter trade-off. - Proc. Natl. Acad. Sci. USA 117: 24893-24899.

Keymer, J.E. 2006. Bacterial metapopulations in nanofabricated landscapes. – Proc. Natl. Acad. Sci. USA 103: 17290-17295.

Koch, A.L. 2001. Oligotrophs versus copiotrophs. - BioEssays 23:657–61.

Kopecky, J. et al. 2014. The effect of antibiotics on associated bacterial community of stored product mites. - PLoS ONE 9: e112919

Lee, C.K. et al. 2016. Evolution of Cell Size Homeostasis and Growth Rate Diversity during Initial Surface Colonization of *Shewanella oneidensis*. - ACS Nano 10:9183-9192.

Legendre, P. and Legendre, L. 2012. Numerical Ecology, 3rd ed. Elsevier, London, pp. 1006.

Margolin, W. 2005. Ftsz and the division of prokaryotic cells and organelles. – Nat. Rev. Mol. Cell Biol. 6: 862–71.

Martins, B.M.C. et al. 2018. Cell size control driven by the circadian clock and environment in cyanobacteria. - Proc. Natl. Acad. Sci. USA 115: E11415-E1142.

Meistertzheim, A.-L. et al. 2016. Patterns of bacteria-host associations suggest different ecological strategies between two reef building cold-water coral species. - Deep Sea Res Part I 114: 12–22.

Michonneau, F. et al. 2016. rotl, an R package to interact with the Open Tree of Life data. - PeerJ Preprints 4:e1471v3.

Nielsen, O. 2004. Mating-Type Control and Differentiation. In: Egel R. (eds) The Molecular Biology of *Schizosaccharomyces pombe*. Springer, Berlin, Heidelberg.

Nieto, C. et al. 2020. Unification of cell division control strategies through continuous rate models. – Phys. Rev. E 101: 022401.

Nobs, J.-B. and Maerkl, S. 2014. Long-term single cell analysis of *S. pombe* on a microfluidic microchemostat array. – PloS ONE 9: e93466.

Paniw, M. et al. 2018. Interactive life-history traits predict sensitivity of plants and animals to temporal autocorrelation. – Ecol. Lett. 21: 275–286.

Paradis, E. et al. 2004. APE: Analyses of phylogenetics and evolution in R language. – Bioinformatics 20: 289–290.

Pottor, T. et al. 2021, Substantial intraspecific variation in energy budgets: Biology or artefact? – Funct. Ecol. 35: 1693-1707.

Priestman, M. et al. 2017. Mycobacteria modify their cell size control under sub-optimal carbon sources. – Front. Cell Dev. Biol. 5:64.

R Core Team (2021) R: A language and environment for statistical computing. R Foundation for Statistical Computing, Vienna, Austria.

Ramin, K.I. and Allison, S.D. 2019. Bacterial tradeoffs in growth rate and extracellular enzymes. – Front. Microbiol. 10: 2956.

Revell, L.J. 2012. phytools: An R package for phylogenetic comparative biology (and other things). - Methods Ecol. Evol. 3: 217–223.

Rochaix, J.-D. 2013. *Chlamydomonas reinhardtii*. In S. Maloy and K. Hughes, editors, Brenner's Encyclopedia of Genetics (Second Edition), pages 521–524. Academic Press, San Diego, second edition.

Rook, G. et al. 2017. Evolution, human-microbe interactions, and life history plasticity. - Lancet 390: 521–30.

Salguero-Gómez, R. et al. 2016. Fast–slow continuum and reproductive strategies structure plant life-history variation worldwide. - Proc. Natl. Acad. Sci. USA 113: 230–235.

Santillan, E. et al. 2019. Trait-based life-history strategies explain succession scenario for complex bacterial communities under varying disturbance. - Environ. Microbiol 21: 3751-3764.

Sauls, J.T. et al. 2016. Adder and a coarse-grained approach to cell size homeostasis in bacteria. – Curr. Opin. Cell Biol. 38: 38–44.

Sauls, J.T. et al. 2019. Control of bacillus subtilis replication initiation during physiological transitions and perturbations. – mBio 10:e02205-19.

Smallegange, I.M. et al. 2014. Correlative changes in life-history variables in response to environmental change in a model organism. – Am. Nat. 183: 784–797.

Smallegange, I.M. et al. 2017. Mechanistic description of population dynamics using dynamic energy budget theory incorporated into integral projection models. - Methods Ecol. Evol. 8: 146-154.

Smallegange, I.M. et al. 2020. Unusually paced life history strategies of marine megafauna drive atypical sensitivities to environmental variability. - Frontiers Mar. Sci. 7:597492.

Steel, C. et al. 2004. Single live cell imaging of chromosomes in chloramphenicol-induced filamentous *Pseudomonas aeruginosa*. - Biochemistry 43: 175–182.

Strovas, T. et al. 2007. Cell-to-cell heterogeneity in growth rate and gene expression in *Methylobacterium extorquens* AM1. – J. Bacteriology 189: 7127–7133.

Sveiczer, A. et al. 1997. The size control of fission yeast revisited. J. Cell Sci. 109: 2947–2957.

Taheri-Araghi, S. et al. 2015. Cell-size control and homeostasis in bacteria. – Curr. Biol. 25:385-391.

Tanaka, M. and Yumura, S. 2021. A 'dynamic adder model' for cell size homeostasis in *Dictyostelium* cells. – Sci. Rep. 11: 13742.

Urushihara, H. and Muramoto, T. 2006. Genes involved in *Dictyostelium discoideum* sexual reproduction. – Europ. J. Cell Biol. 85: 961–968.

Vitova, M. et al. 2010. *Chlamydomonas reinhardtii*: Duration of its cell cycle and phases at growth rates affected by light intensity. - Planta 233: 75–86.

Vrieze, de Groot, P.F. et al. 2013. Fecal transplant: A safe and sustainable clinical therapy for restoring intestinal microbial balance in human disease? - Best Pract. Res. Clin. Gastroenterol. 27: 127-137.

Wallen, R. and Perlin, M. 2018. An overview of the function and maintenance of sexual reproduction in dikaryotic fungi. - Frontiers Microbiol. 9: 503.

Zheng, H. et al. 2016. Interrogating the *Escherichia coli* cell cycle by cell dimension perturbations. - Proc. Natl. Acad. Sci. USA 113: 15000-15005.

Zindel, R. et al. 2017. The role of the bacterial community in the nutritional ecology of the bulb mite *Rhizoglyphus robini* (Acari: Astignmata: Acaridae). - FASEB J. 27: 1488-1497.

Table 1. Model parameters for the 13 microorganisms (see also Fig. 1A). Parameters are expected feeding level $E(Y)$, the fraction of assimilated energy allocated to respiration, κ, cell length at birth, L_b, length at division, L_d, maximum length, L_m, mortality rate, μ, von Bertalanffy growth rate, $\dot{r}_B$, and number of offspring produced, n_O. Units are in brackets. Superscript numbers are references (see footnotes below). Species numbers are the same as in the Fig. 1. See further main text.

			Model parameters							
	Species	**Kingdom**	**E(Y)**	**κ**	L_b	L_d	L_m	**μ**	n_O	$\dot{r}_B$
			(–)	**(–)**	**(μm)**	**(μm)**	**(μm)**	**(h^{-1})**	**(#)**	**(h^{-1})**
1	*Dictyostelium discoideum*	Protista	0.80	0.90	15.26 [p]	24.74 [p]	48.48 [p]	0.01	2	0.12
2	*Chlamydomonas reinhardtii*	Plants	1.00	0.90	12.64 [q]	27.26 [q]	29.23 [q]	0.01	2	0.03
3	*Bacillus subtilis*	Bacteria	0.30	0.90	3.84 [l]	6.89 [l]	13.87 [l]	0.01	2	1.62
4	*Synechococcus elongatus*	Bacteria	1.00	0.90	2.04 [o]	5.98 [o]	8.031 [o]	0.01	2	0.03
5	*Mycobacterium smegmatis*	Bacteria	0.80	0.90	5.06 [e]	8.72 [e]	11.96 [f]	0.01	2	0.09
6	*Pseudomonas aeruginosa*	Bacteria	0.80	0.90	3.86 [i]	17.34 [i]	26.00 [j]	0.01	2	0.25
7	*Shewanella oneidensis*	Bacteria	0.80	0.90	1.35 [k]	3.35 [k]	5.00 [k]	0.01	2	0.17
8	*Escherichia coli*	Bacteria	0.50	0.90	2.18 [g]	3.46 [g]	8.00 [h]	0.01	2	5.21
9	*Caulobacter vibrioides*	Bacteria	0.70	0.90	1.76 [m]	3.22 [m]	5.30 [n]	0.01	2	1.10
10	*Methylorubrum extorquens*	Bacteria	0.90	0.90	1.71 [r]	4.40 [r]	5.24 [r]	0.01	2	0.15
11	*Desulfovibrio vulgaris*	Bacteria	1.00	0.90	3.15 [s]	6.18 [s]	6.19 [s]	0.01	2	0.49
12	*Schizosaccharomyces pombe*	Fungi	0.90	0.90	8.67 [a]	16.00 [a]	19.43 [b]	0.01	2	0.69
13	*Saccharomyces cerevisiae*	Fungi	0.99	0.90	3.78 [c]	8.12 [c]	8.24 [d]	0.01	2	0.56

[a] Buchwald and Sveiczer (2006); Sveiczer et al., (1997); [b] Nobs and Maerkl (2014); [c] Ferrezuelo et al., (2012); [d] Allard et al., (2018); [e] Priestman et al., (2017); [f] Aldridge et al., (2011); [g] Nieto et al., (2020); [h] Zheng et al., (2016); [i] Deforet et al., (2015); [j] Steel et al., (2004) [k] Lee et al., (2016); [l] Sauls et al., (2019); [m] Banerjee et al., (2017); [n] Beaufay et al., (2015); [o] Martins et al., (2018); [p] Tanaka and Yumura (2021); [q] Vitova et al., (2010); [r] Strovas et al., (2007); [s] Fiévet et al., (2015).

In case of *S. cerevisiae*, we calculated cell length as the cell diameter $2r$ (μm) from cell volume V (μm^3), assuming *S. cerevisiae* cells are sphere-shaped so that $V = \frac{4}{3}\pi r^3$, from which follows that cell length equals $2r = 2\sqrt[3]{\frac{3}{4}\pi V}$. To calculate L_m for *S. cerevisiae*, we used the volume of a mother cell and bud (Allard et al., 2018), and subtracted the volume of the mother cell at division from the volume of the mother cell at birth, assuming that the size at birth of the mother equals the bud's size. Cell length of the mother and bud were calculated from the volume measures as before, and added together to give maximum length, L_m, of *S. cerevisiae*. In case of *Chlamydomonas reinhardtii*, we assumed that, given their shape, cells were proportioned as 4 × 4 × 10 μm (Rochaix 2013). Given the fact that cell volume $V = \frac{4}{3}\pi r^3$ and $r^3 = 4a \cdot 4a \cdot 10a$, gives cell length as $10a = \sqrt[3]{3V/(640\pi)}$. In case of *Mycobacterium smegmatis*, measures of cell length at birth and the elongated length of a single cell were combined to give L_m. In case of *Pseudomonas aeruginosa*, only log values of cell length were available (Deforet et al., 2015), which we backtransformed. Cell length measures of *Bacillus subtilis* were available for different media, and we used those values obtained for cells grown on a favourable, glycerol rich medium (Sauls et al.,

2019). In case of *Dictyostelium discoideum*, we inferred from photos that cells are circle-shaped in between birth and mitosis (Tanaka and Yumura, 2021), so that cell surface $S = \pi r^2$, from which follows that the cell length equals $2r = 2\sqrt{S/\pi}$. Cell surfaces measures to calculate cell lengths of *D. discoideum* were taken from two time frame photos taken between mitosis and birth (Tanaka and Yumura, 2021). Finally, we manually measured cell lengths of *Desulfovibrio vulgaris* from a series of scale-barred images of cell length over time (Fiévet et al., 2015). For all species, we estimated the von Bertalanffy growth rate, $\dot{r}_B$, using a nonlinear least-squares estimation procedure in R (nls function) (R Core Team 2021) to fit the equation $L_t = L_d - [L_d - L_b]e^{-\dot{r}_B t}$ for $\dot{r}_B$ (Smallegange et al., 2017) against observed growth curves of cell length L_t (µm) over time t (hours), taken from the literature (see R code in Supplementary Material).

Table 2. DEB-IPM predictions on the derived life history trait population growth rate λ (h^{-1}) mean lifetime reproductive success R_0 (no h^{-1}) and generation time T (h) (see main text). Parameters are: length at division, L_d, and maximum length, L_m. Species numbers are the same as in Fig. 1.

	Species	**Derived life history trait**		
		λ	R_0	T
1	*Dictyostelium discoideum*	1.08	1.86	7.83
2	*Chlamydomonas reinhardtii*	1.17	1.93	4.24
3	*Bacillus subtilis*	1.03	1.71	16.42
4	*Synechococcus elongatus*	1.08	1.87	7.93
5	*Mycobacterium smegmatis*	1.00	0.91	79.81
6	*Pseudomonas aeruginosa*	1.11	1.90	6.22
7	*Shewanella oneidensis*	1.35	1.97	2.27
8	*Escherichia coli*	1.07	1.85	8.52
9	*Caulobacter vibrioides*	1.02	1.63	21.50
10	*Methylorubrum extorquens*	1.06	1.82	10.28
11	*Desulfovibrio vulgaris*	1.01	1.41	36.04
12	*Schizosaccharomyces pombe*	1.37	1.98	2.16
13	*Saccharomyces cerevisiae*	1.26	1.96	2.88

Figure 1.

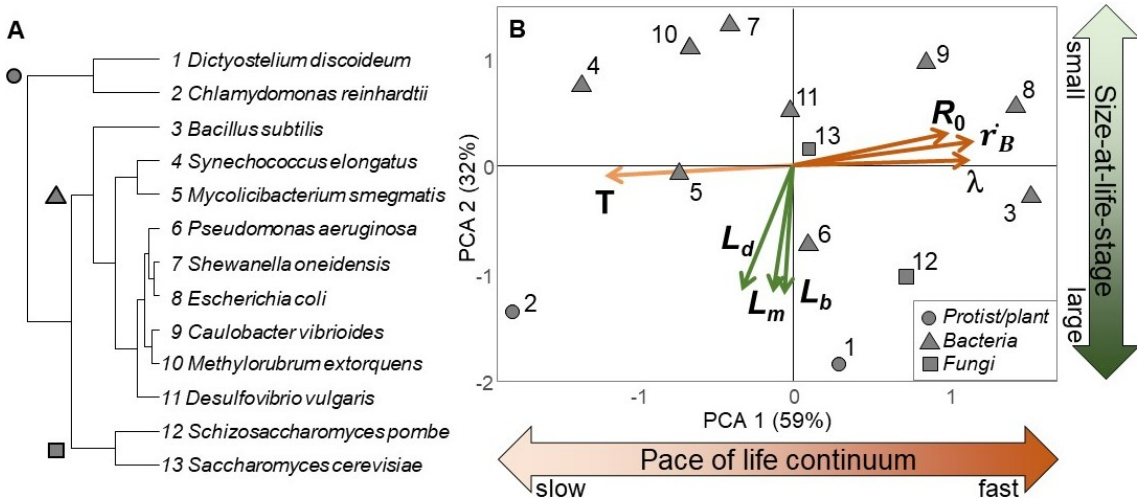

Figure 1. Life histories of microorganisms are structured along the pace of life continuum (fast–slow continuum) and a size-at-life-stage continuum. **(A)** Phylogenetic tree of the 13 study species created using the *rotl* package (Michonneau et al., 2016) to download a tree from the Open Tree of Life (OTL) (Hinchliff et al., 2015), after taxonomical updating using the R library *taxize* (Chamberlain and Szocs, 2013) (input names of *Synechococcus elongatus*, *P. aeruginosa* and *Escherichia coli* were changed to *Synechoccocus elongatus* CCMP1630, *Pseudomonas aeruginosa* 148 and *Escherichia coli* 402290, respectively). Branch length was computed using the *compute.brlen* in the R package *ape* (Paradis et al., 2004). Polytomies were collapsed using the function *multi2di* in *ape* (Hinchliff et al., 2015). **(B)** To characterise life histories, a phylogenetically informed PCA was performed on cell length at birth, L_b, length at division, L_d, maximum length, L_m, the von Bertalanffy growth rate, $\dot{r}_B$, population growth rate (λ), mean lifetime reproductive success (R_0) and generation time (T). We kept the first two PCA axes, because their associated eigenvalues were > 1 (following the Kaiser criterion [Legendre and Legendre, 2012]: $\lambda_{axis\ 1} = 17.04$; $\lambda_{axis\ 2} = 5.00$; $\lambda_{axis\ 3} = 0.20$). Arrow lengths are proportional to the loadings of each trait onto these two axes. Circles in (A) and (B) indicate protist or plant, triangles in (A) and (B) indicate bacteria, and squares in (A) and (B) indicate fungi. Numbers next to symbols in (B) identify species according to numbers in (A) and in Tables 1 and 2.